Proceedings of ICFA Mini-Workshop on Impedances and Beam Instabilities in Particle Accelerators, Benevento, Italy, 18-22 September 2017, CERN Yellow Reports: Conference Proceedings, Vol. 1/2018, CERN-2018-003-CP (CERN, Geneva, 2018)

DESIGN OF LOW-IMPACT IMPEDANCE DEVICES: THE NEW PROTON SYNCHROTRON BOOSTER ABSORBER SCRAPER (PSBAS)*

L. Teofili†,1,2, I. Lamas, T. L. Rijoff, CERN, Geneva, Switzerland
M. Migliorati[2], University of Rome La Sapienza, Rome, Italy
[1] also at University of Rome La Sapienza, Rome, Italy; [2] also at INFN, Rome, Italy

Abstract

At CERN the HL-LHC (High Luminosity Large Hadron Collider) and the LIU (LHC Injection Upgrade) projects call for an increase in beam parameters such as energy, intensity and brightness. To achieve this goal the whole accelerator complex will be upgraded. Systems, equipment and devices need to be redesigned and rebuilt accounting for the demanding new beam features. In this framework device impedance is a key parameter. It is essential to evaluate and to minimize the impedance of the component during its early design phase. This avoids beam instabilities and minimizes beam losses and induced heating. In this paper we outline general guidelines for a low-impedance design and we show how to implement them in a real case, taking as example the design of the new Proton Synchrotron Booster Absorber Scraper (PSBAS). This is a key component aimed to remove the beam halo at the beginning of the LHC accelerator chain.

INTRODUCTION

During the coming years the CERN accelerator complex will be upgraded to improve its performance. An increase of the beam energy, intensity and brightness is foreseen in the framework of the projects LIU (LHC Injection Upgrade) [1] and HL-LHC (High Luminosity Large Hadron Collider) [2]. A large number of systems, equipment and devices will be redesigned taking into account the challenging new situation. Particularly, the raised intensity of the HL-LHC beams may lead to beam instabilities and high RF-heating. Thus, extra attention need to be given to electromagnetic and thermo-mechanical interactions between the beam and its surroundings. In this context, the electromagnetic beam-device coupling index, the device impedance, is becoming an increasingly important parameter. Its evaluation and minimization is essential during the device design phase to avoid beam instabilities and reduce beam losses and induced heating.

Geometrical features that lead to high impedance are well known by the impedance working community along with the way to cure them [3], [4]. However, little has been written on how to implement such curing methods on the design of real components. Such a task is far from being trivial since real components have to fulfill also other requirements as easy manufacturing and integration or size and cost constraints.

Thus, in the first part of this paper, we review the main geometric high impedance features most commonly encountered in device designs and the way to cure them. Subsequently, taking as an example the design of the new Proton Synchrotron Booster Absorber Scraper (PSBAS), a key component aimed to remove the beam halo at the beginning of the LHC accelerator chain, we show how to apply these curing methods to realize the low impedance design of a real device.

METHODOLOGY

For the current investigation a careful analysis of the designs of various mechanical devices under development at CERN was carried out. It focused on the components directly exposed to the beam which are to be installed inside the synchrotrons, Proton Synchrotron Booster (PSB), Proton Synchrotron (PS), and Super Proton Synchrotron (SPS), or in the collider (LHC). For them impedance play a key role. Some of these devices, in their preliminary design, exhibited common geometric high-impedance features, well documented in literature [3], [4]. This could have potentially led to harmful consequences for the beam and for the device-itself. The high impedance geometric configurations were deeply investigated through numerical simulations with the aim of eliminating them or reducing their effects with simple and cost-effective modifications to the device design. They were considered individually and modelled in the CAD (computer aided design) tool of a Finite Integration Technique (FIT) software. Their basic geometrical quantity were considered as parameters in order to characterize the effects of their variation. In this work only the longitudinal impedance is discussed since, usually, solving it reduces also the transverse impedance. A careful analysis of the transverse impedance is left to future studies. The software used for simulations was CST Particle Studio® [5]; its time domain solver, Wakefield [6], is a well known and tested tool at CERN for device impedance computation [7], [8]. The knowledge acquired during these analysis was subsequently applied to enhance the impedance performances of the device with high impedance.

RESULTS: GENERAL GUIDELINES AND THE PSBAS CASE

In this section, initially, we present the three most common geometric high-impedance features found in most preliminary device designs. Their effects are analyzed and a possible simple and cost-effective design modification to eliminate them, or at least to reduce their detrimental impact, is proposed. Subsequently, as an example of real application of these curing modifications the design evolution of the PSBAS is presented.

* Work supported by LHC Injection Upgrade (LIU) project
† lorenzo.teofili@uniroma.it

https://doi.org/10.23732/CYRCP-2018-001.111

Abrupt Changes of Section in Components

Abrupt changes of section were often recurring in the preliminary design of the analyzed devices. However, they should be avoided because they generate electromagnetic trapped modes (HOM) visible as well defined peaks in the impedance curve, (refer to Fig. 2).

In order to investigate abrupt changes of section effects, the geometry shown in Fig. 1 was simulated. The radius of the small pipe was considered fixed (r_a = 5 mm) while the radius of the larger pipe, r_b was parametrized. Compared to the case $r_a = r_b$, i.e. no section changes, for $r_b > r_a$ an increase in the impedance can be observed. In the case r_b = 10 mm no trapped modes are visible at the investigated frequencies, i.e. no peaks are present in Fig. 2. However, the same Fig. 2 shows that for $r_b \geq 35$ mm trapped modes start to appear. Further, the more r_b increases the more the observed modes shift to lower frequencies raising their impedance peak value. This finding agrees with well known results, [3], that shown how for an abrupt change of section between two pipes the key parameter is the pipes radii ratio r_b/r_a. By increasing it, the frequency of the resonant modes decreases while their impedance peak value increases.

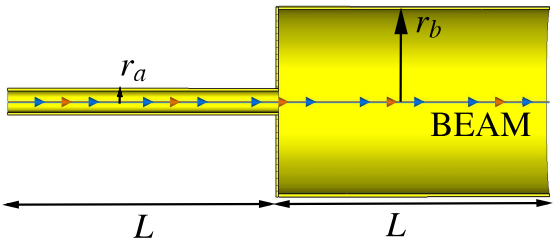

Figure 1: Abrupt section change geometry model: r_a = 5 mm, L = 100 mm, r_b = parametrized.

An easy solution to the problem is tapering. To investigate its effects, the geometry of Fig. 1 was modified, adding a conical connection of length L_t between the two pipes as illustrated in Fig. 3. The radius of the small pipe, the length of the pipes and the length of the conical taper were considered fixed (r_a = 5 mm, L = 100 mm, L_t = 50 mm) while the radius of the larger pipe, r_b was parametrized. The results of the simulations are reported in Fig. 4. In the case $r_b > r_a$ there is an impedance increase in comparison to the case $r_a = r_b$, i.e. no section changes. The non tapered configuration has the same qualitative behaviour. For r_b = 10 mm no trapped modes are visible at the investigated frequencies, in this case virtually no differences can be found between tapered and not tapered configurations. As for the configuration without taper (Fig. 2) for $r_b \geq 35$ mm trapped modes start to appear, although the beneficial effects of the taper results in lower impedance peak values. This can be clearly seen comparing the results of the abrupt section change geometry (Fig. 2) with the ones of the tapered configuration (Fig. 4). Further, considering the r_b value which leads to the worst case scenario (i.e. the highest r_b considered) we investigated the effects of variation in the taper length. The result is shown with a dashed line in Fig. 4, revealing the beneficial effects of a longer taper which further decrease the peak impedance of the modes.

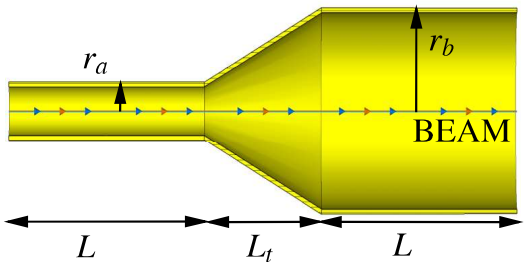

Figure 3: Tapered section change geometry model: r_a = 5 mm, L = 100 mm, L_t = 50 mm, r_b = parametrized.

Gaps

Gaps and absence of electrical connections among components were another, quite common, high impedance feature found in the preliminary designs analyzed. Gaps should be avoided because they create capacitive effects leading to

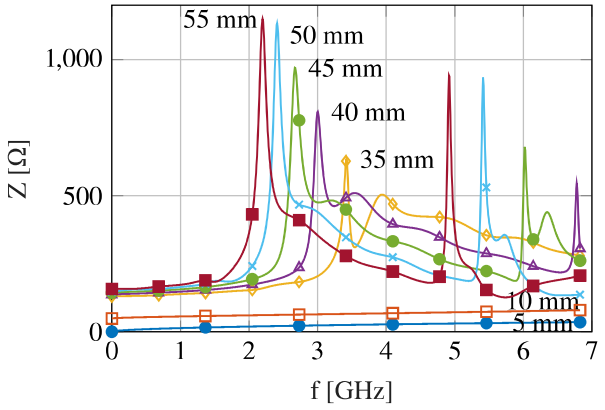

Figure 2: Abrupt section change configuration. Longitudinal impedance modulus computed for different values of r_b.

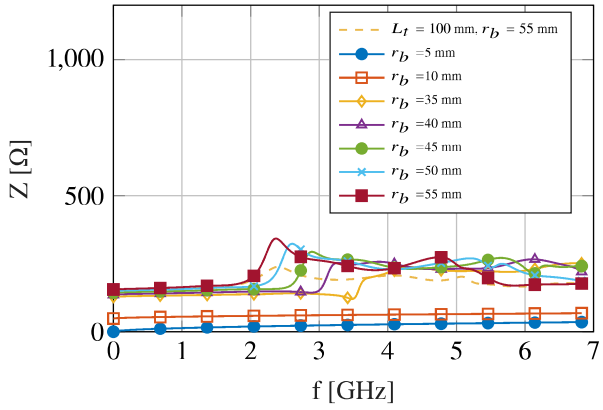

Figure 4: Tapered section change configuration. Longitudinal impedance modulus for different values of r_b.

high impedance values at low frequencies, which are very dangerous for RF heating [9]. In order to study their effects the geometry shown in Fig. 5 was simulated. The length and the radius of the pipes were considered fixed (r = 5 mm and L = 100 mm) while the gap between the pipes, g, was parametrized.

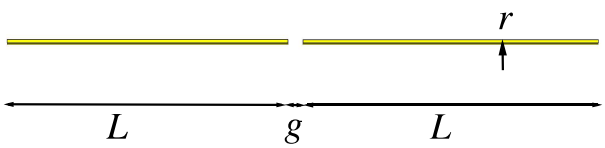

Figure 5: Open gap model geometry: r = 5 mm, L = 100 mm, g = parametrized.

Impedance simulations results are reported in Fig. 6 for different values of g. The capacitive effects of the gap results in high impedance at very low frequencies. The impedance peaks values increase with the distance between the pipes. This is consistent with the results obtained in [4]. Other peaks at higher frequency can be seen from Fig. 6. According to [4], they map trapped modes in the gap.

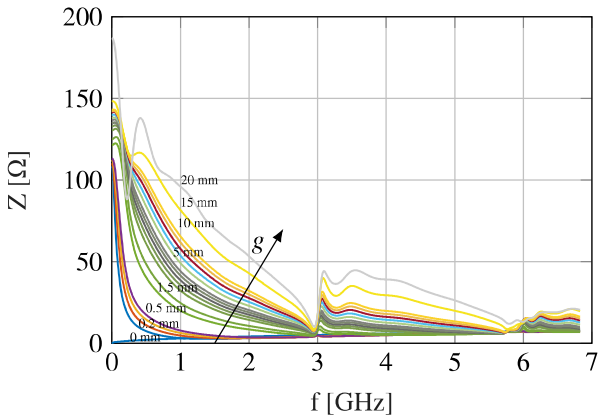

Figure 6: Open gap model geometry, longitudinal impedance modulus computed for different values of g.

The easy solution to the detrimental effects of a gap is the gap elimination by connections. Figure 7 shows the same geometrical layout of Fig. 5 with the addition of two symmetrical electrical connections between the two pipes. For simulations the length and the radius of the pipes were considered fixed (r = 5 mm and L = 100 mm) while the gap between the pipe, g, was parametrized. The obtained results, reported in Fig. 8, demonstrate the effectiveness of applying connections. Comparing the impedance of the open gap geometry, Fig. 6, with the impedance of the same geometry with connections, Fig. 8, one notices that impedance at very low frequencies is drastically reduced for all gap sizes when connections are added. However, in the connected geometry a new trapped mode is present, around 2 GHz. It was not found in the open gap configuration. No shown results demonstrate that it strongly depends on the contacts shape and on the number of connection points. This resonant mode can be shifted to higher frequencies simply adding more connections. Impedance behaviour for frequencies higher than 3 GHz seems not to be affected by the connection. Comparing the results shown in Fig. 6 and Fig. 8 a similar trend can be observed in this range.

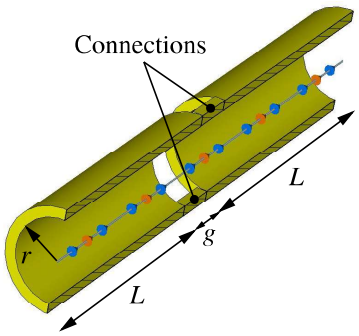

Figure 7: Gap with connections model geometry: r = 5 mm, L = 100 mm, g = parametrized.

Parasitic Cavities

The last high impedance feature noticed during the design analysis was the presency of parasitic cavities. Every empty volume that is directly seen by the beam potentially behaves like a parasitic cavity, i.e. it extract energy from the beam in order to excite its resonant modes. This leads to really high peaks in the impedance curve of the device and it is very dangerous due to long range instability effects [10]. It is well recognized in literature that in the case of a cavity a key role is played by the wall material, particularly the electrical conductivity σ strongly influences the peak impedance of the mode. The cavity geometry shown in Fig. 9 was simulated considering different wall materials.

The impedance modulus of the mode that resonates at the lowest frequency is reported in Fig. 10, where only a small range of frequencies around the mode has been considered.

The most common way to solve this problem is the use of RF-shieldings. RF-shielding is a metal screen that blocks

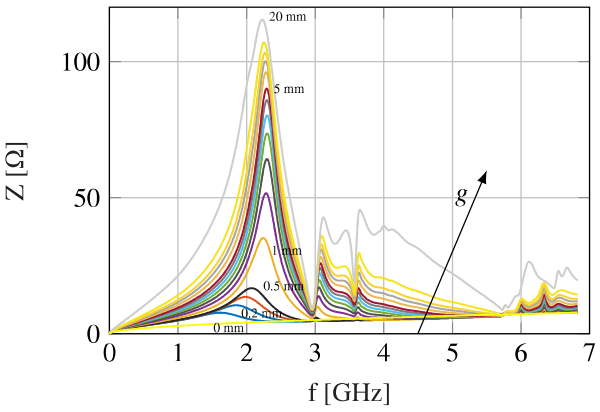

Figure 8: Gap with connection model geometry. Longitudinal impedance modulus for different values of g.

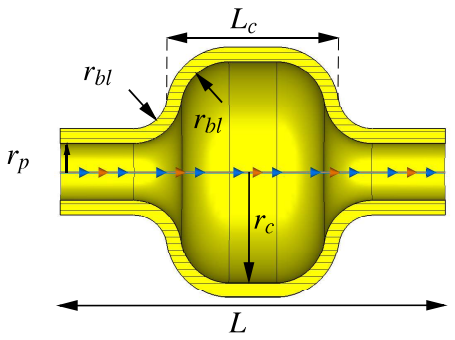

Figure 9: Unshielded cavity geometry: r_p = 60 mm, L = 800 mm, r_{bl} = 100 mm, L_c = 300 mm, r_c = 230 mm.

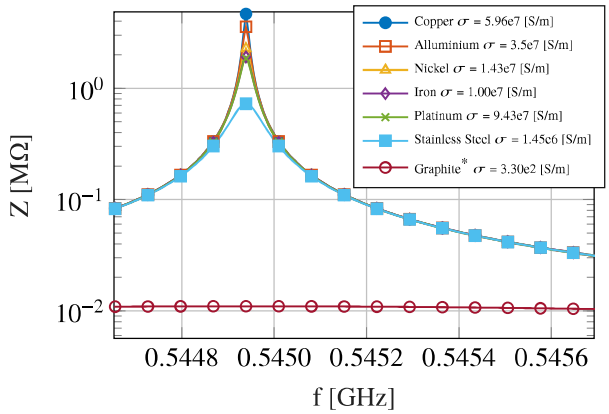

Figure 10: Unshielded cavity geometry. Longitudinal impedance computed for different values of the material electrical conductivity σ. Logarithmic scale.

electromagnetic interactions between the beam and the empty volume. The RF-shielding can have different shapes in order to better fit the geometry they have to shield. An example of shielding is proposed in Fig. 11, where the geometry of the previous parasitic cavity (refer to Fig. 9) has been modified adding ten metallic tubes on a circle connecting the inner pipe with the outer one.

The results of the electromagnetic simulations on the shielded cavity geometry (Fig. 12) show a striking impedance reduction of about 6 orders of magnitude if compared with the results of the no-shielded configuration in Fig. 12 due to the fact that the resonant mode has disappeared.

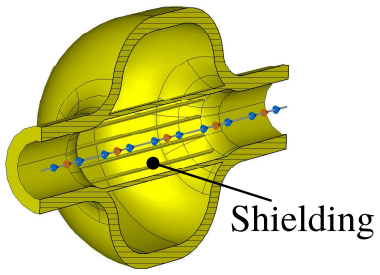

Figure 11: Shielded cavity geometry model.

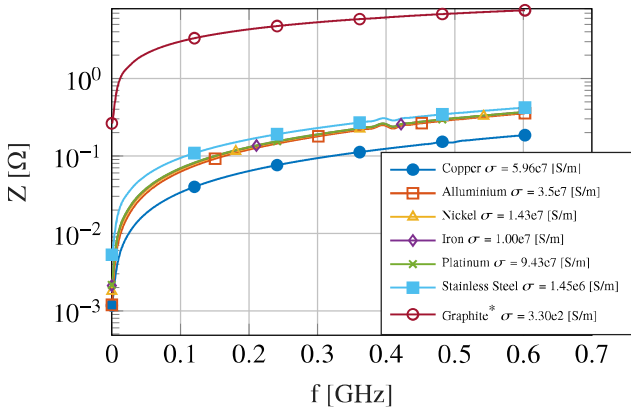

Figure 12: Shielded cavity geometry. Longitudinal impedance modulus computed for different values of the material electrical conductivity σ. Logarithmic scale.

The PSBAS case

As discussed previously, the outlined general guidelines need to be used in order to improve impedance performances in poor devices. In the following, as an example of their application, we summarize the evolution of the PSBAS design from the preliminary high impedance design to the final low impedance one.

The PSB scraper (refer to Fig. 13) is a device to be installed in the PSB at CERN. Its purpose is to clean the beam halo, at the very early stage of acceleration, absorbing it in two graphite blocks. Due to particular application needs, two working configurations were required: movable mask in and movable mask out, Fig. 13b. This led to the design of a movable central part.

The electromagnetic properties of the equipment were assessed through simulations with CST Particle Studio®. According to the simulation results, we iterated on the mechanical design applying the previously outlined low impedance design guidelines in order to obtain the final low impedance design. The high impedance characteristics of the PSBAS preliminary design are shown in Fig. 13c on the CST simulated model. In the preliminary PSBAS design, shown in Fig. 13a and 13b, impedance mitigation measurements were already taken: the replacement vacuum chamber was acting as a shielding against the vacuum tank, a potential parasitic cavity, preventing it from resonating. However, they were not sufficient and the impedance behaviour of the device was unacceptable. To allow an easy motion of the movable graphite mask, the latter was not electrically connected to the rest of the device along the beam path direction. Thus, gaps were presents in this design, leading to the generation of high order modes, trapped there. Moreover, such a design presents an unshielded empty volume around the fixed graphite mask. The discussed features generated trapped modes at frequencies lower than 0.4 GHz. The latter is considered as the acceptable lower limits for HOMs in the PSB machine [11].

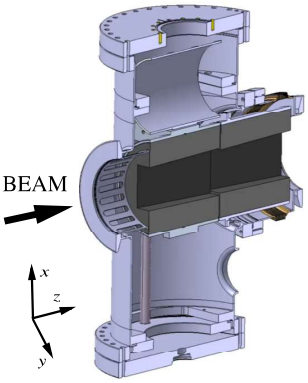

(a) Preliminary PSBAS design: Isometric view.

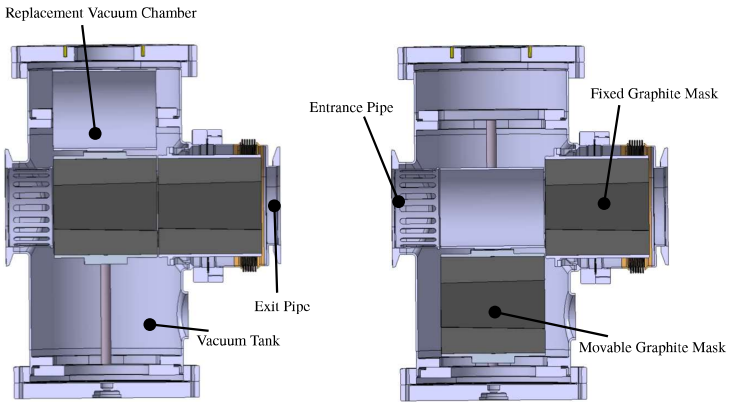

(b) Preliminary PSBAS design: Working configuration and nomenclature

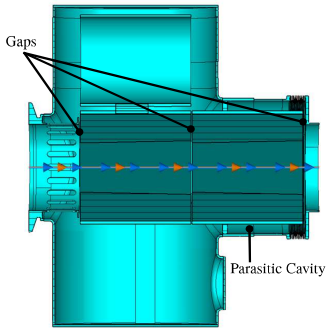

(c) Preliminary PSBAS design: CST model and high impedance features.

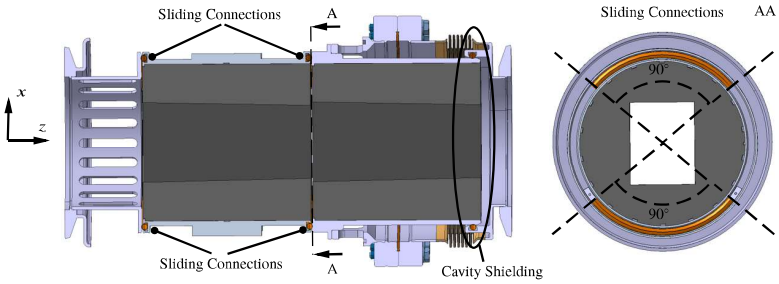

(d) Final low impedance PSBAS design: Section view and particular.

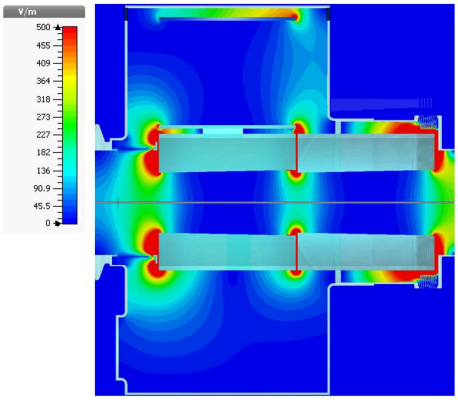

(e) PSBAS preliminary design, electric modes field shapes

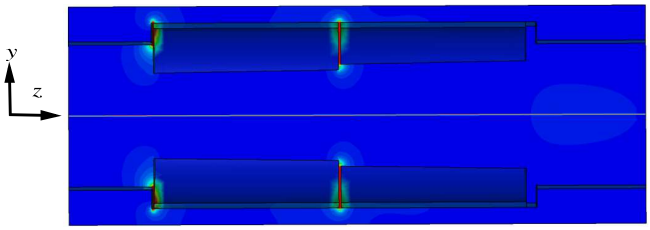

(f) PSBAS final design, electric modes field shapes (scale on Fig. 13e)

Figure 13: Different Geometries of the PSBAS: preliminary and final low impedance design

Therefore, the preliminary PSBAS design, with an HOM at 1.8 GHz, was not impedance compliant. The results of the electromagnetic simulations, electric modes field shapes and device impedance, are shown in Fig. 13e and 14.

The preliminary design was subsequently modified as shown in Fig. 13d:

- Electric sliding connections between movable and fixed parts were added to eliminate the gap effects.
- The parasitic cavity was shielded by a geometrical modification.

This led to an impedance compliant design, eliminating the modes at low frequencies and decreasing the impedance of the device of three orders of magnitude if compared with the previous performances. The results of the electromagnetic simulations, field shapes of the electric modes and device impedance, are shown in Fig. 13f and 14. Please note that in both the final and preliminary PSBAS design there are abrupt changes of section between the graphite masks and the pipes. No attenuation method was applied to reduce their effects because, due to operational and space

constraints, it was impossible to add taper. However, the contribution of the section changes is negligible.

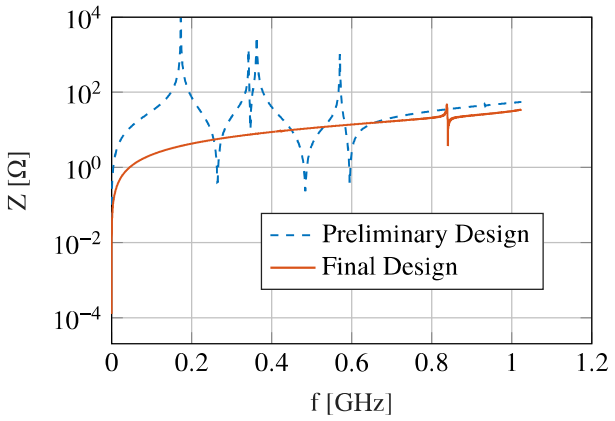

Figure 14: PSBAS final vs PSBAS preliminary design, Longitudinal Impedance Modulus. Logarithmic scale.

CONCLUSION

Prior work has documented the importance of reducing the impedance of accelerator devices and so of the whole machine [3], [8]. However, the majority of the previous studies focus on the impedance induced effects on the beam dynamics. They show geometric configurations that lead to a high impedance device and suggest cure methods, however, most of the time these approaches remain unapplied in a real case, thus ignoring limitations such as device component motion, space constraints, costs etc. In this paper, we reviewed the most common high impedance geometric features usually present in a preliminary device design and simple and cost-effective way of modifying geometries to obtain low impedance designs. Subsequently, we showed how to apply these methods to improve the impedance performance of a real, complex, device, the Proton Synchrotron Booster Absorber Scraper. We obtained a striking impedance reduction between the preliminary and the final design of almost three orders of magnitude with small increase in cost and complexity of the device itself. Therefore, this study indicates that, considering since the beginning not only mechanical and operational requirements, but also impedance requirements, it is possible to produce low impedance - cost effective components without affecting their main functionalities. This is a key approach for the conception of components for the LIU project and will be even more important for future hadron accelerators which are likely to have even higher intensity and lower emittance beams.

REFERENCES

[1] J. Coupard *et al.*, "LHC Injectors Upgrade Projects at CERN", in *Proc. 7th Int. Particle Accelerator Conf. (IPAC'16)*, Busan, Korea, May 2016, paper MOPOY059, pp. 992–995.

[2] G. Apollinari, A. Bejar, O. Bruning, M. Lamont, L. Rossi, "High-Luminosity Large Hadron Collider (HL-LHC) : Preliminary Design Report", CERN, Geneva, Switzerland, Rep. CERN-2015-005, Dec. 2015.

[3] L. Palumbo, V. G. Vaccaro, "Wake Fields and Impedance", in *Proc. CERN Accelerator School (CAS)*, Eger, Hungary, 1995, paper LNF-94/041 (P), pp. 331–390.

[4] Y. Shobuda, Y. H. Chin and K. Takata, "Coupling impedances of a gap in vacuum chamber", *Phys. Rev. ST Accel. Beams*, vol. 10, no. 4, p. 044403, Apr. 2007.

[5] CST Studio Suite, `https://www.cst.com/products/csts2`

[6] CST Studio Suite: Eigenmode Solver, `https://www.cst.com/products/cstmws/solvers/eigenmodesolver`

[7] C. Zannini, "Electromagnetic Simulation of CERN accelerator Components and Experimental Applications", Ph.D. thesis, Phys. Dept., Ecole Polytechnique, Lausanne, Switzerland, 2010.

[8] B. Salvant, "Impedance model of the CERN SPS and aspects of LHC single-bunch stability", Ph.D. thesis, Phys. Dept., Ecole Polytechnique, Lausanne, Switzerland, 2013.

[9] M. Furman, H. Lee and B. Zotter, "Energy loss of bunched beams in RF cavities", Lawrence Berkeley Laboratory, Berkeley, California, Rep. SSC-086, 1986.

[10] K. Ng, *Physics of intensity dependent beam instabilities*: World Scientific, 2006.

[11] Updated status of the PSB impedance model, `https://indico.cern.ch/event/319950/contributions/740766/\\attachments/616601/848489/PSB_impedance_model_update.pdf`